EFFECT OF LOCAL CELLULAR TRANSFORMATION ON FATIGUE SMALL CRACK GROWTH IN CMSX-4 AND CMSX-2 AT HIGH TEMPERATURE.
- For Refurbishment Technology -

Masakazu Okazaki, Tomoyuki Hiura and Toshio Suzuki

Department of Metallurgy, School of Engineering
The University of Tokyo
Hongo 7-3-1, Bunkyou-ku, Tokyo 113-8656
JAPAN

Abstract

In order to get fundamental understanding to establish a refurbishment technology for advanced gas turbine components, the cellular formation associated with a γ/γ' microstructure coarsened in lamellar or equiaxed arrays in single crystal Ni-base superalloys, CMSX-2 and CMSX-4, have been studied, supposing the case in which they were previously subjected to a damage associated with local plastic deformation, followed by a re-heat treatment. During this study special attention was paid to understand the nucleation and the growth of the transformation from viewpoints of crystallo-plasticity and thermo dynamics. The experimental evidence indicated that the transformation originated and developed with high anisotropy, being influenced by the following factors: the strain field produced by local plastic deformation, the crystallographic orientation, the re-heat treatment temperature and time, and the microsegregation in the material. It was shown that the transformation was reproduced in material previously subjected to fatigue and thermo-mechanical fatigue damage, in which the shearing of γ' precipitates resulting from the activation of $\{111\}\langle 1\bar{1}0\rangle$ slip systems was significant. It was shown that diffusion was controlling the growth rate of the transformation, accompanied with an activation energy of 36 kcal/mol. Furthermore, the effect of the local cellular transformation on the high temperature small fatigue crack propagation was quantified experimentally.

Superalloys 2000
Edited by T.M. Pollock, R.D. Kissinger, R.R. Bowman,
K.A. Green, M. McLean, S. Olson, and J.J. Schirra
TMS (The Minerals, Metals & Materials Society), 2000

Introduction

Recently industrial gas turbine power plant have been the major baseload source of power for many countries. These applications require a highly reliable, long-term load machine which can operate using cheap, available fuels [1]. Nobody doubts that the directions of the development are not only to achieve high thermal efficiency but also cost reduction for production and maintenance. Thus, repair, recoating and refurbishment technology of the hot section components in service under extremely severe conditions will be inevitable in very near future. Nevertheless, no standards, or no sophisticated technologies have not been established yet.

As an example, let us suppose a simple refurbishment process in which single crystal alloys have been subjected to actual damage (e.g., fatigue, creep-fatigue and thermo-mechanical fatigue) during the servicing period and then a reheat treatment is given for damage recovery as is normal for pollycrystalline alloys. What re-heat treatment should be given ? Is the same treatment condition as for the virgin material applicable ? Is there a problem of local recrystallization in this case ? There seems to be little understanding on the above factors. Some researchers have studied the phenomenon of local recrystallization and abnormal precipitate growth [2-5]. According to these investigations, abnormally growing cellular microstructures are found to occur. Because single crystal alloys are generally free from grain boundaries strengthening elements, it is not difficult to suppose harmful effects on the mechanical properties, once local or general recrystallization is reached. This may not be unusual. For example, a shot blasting procedure on Ni-based superalloys before coating, which is often conducted to improve the adhesion between the film/substrate, is also a straining process [2]. More recently, Walston et al. [5] have studied microstructural instability in the second and third generation single crystal superalloys including higher levels of refractory elements, or the precipitation of Topologically Close Packed (TCP) phases. They have confirmed that local straining due to shot-blasting accelerated the transformation accompanied with TCP phase formation at the substrate/coating film interface, and that it could result in significant reduction of creep properties. What happens in these kinds of superalloys when exposed to fatigue, creep-fatigue and thermo-mechanical fatigue damage ? Note that these damages are more or less associated with plastic deformation.

This work has been conducted to clarify the factors leading to the abnormal microstructure, or cellular transformation, resulting from the local plastic deformation in single crystal Ni-base superalloys, CMSX-2 and CMSX-4. During the study special attention was paid to understand the nucleation and growth behavior from viewpoints of crystallography and thermo dynamics. The relationship between the transformation and the actual failure damage was also explored. Furthermore, the effect of the local cellular transformation on high temperature fatigue strength was investigated.

Materials

The materials tested in this work are single crystal Ni-base superalloy, CMSX-4 and CMSX-2. The chemical compositions and the conditions of heat treatments are given in Table I. At the stage of the heat treatments, the volume fraction and the size of cubic γ' precipitates are about 0.5 μm and 65 % in the former, and 0.5 μm and 62 % in the latter.

Results

Outline on Formation of Cellular Microstructure.

What can happen in the single crystal alloys from a metallurgical viewpoint, when they receive refurbishment and recoating processing after a service period ? In order to

TABLE I: Chemical Compositions and The Conditions of Heat Treatments.

Chemical compositions (wt. %)

	Cr	Co	Mo	W	Ti	Ta	Re	Hf	Al	Ni
CMSX-4	6.4	9.7	0.6	6.4	1.0	6.5	2.9	0.1	5.7	bal.
CMSX-2	7.9	4.6	0.6	7.9	1.0	-	-	0.1	5.6	bal.

Heat treatments:
CMSX-2: 1250℃x 15 min. +1276℃x2 h.+ 1296℃x3 h. → Ar. F.C.
1080℃x 4 h. → Ar. F.C. .....870℃x 4 h.→ A.C.
CMSX-4: 1277℃x 2 h. +1288℃x 2 h.+ 1296℃ x 3 h. + 1304℃x 3 h. + 1313℃ x2 h.
+1316℃x 2 h. + 1318℃ x2 h. + 1321℃ x2 h. → Ar. F.C.
1140℃ x 6 h. → Ar. F.C. .....870℃ x 20 h. → A.C.

TABLE II: Conditions of Reheat Treatments.

	Reheat treatment	Aging treatment
Condition A	1080 ℃x 20 hr.*	1080 ℃x 4 hr. + 870 ℃x 4 hr.*
Condition B	1220 ℃x 1.5 hr.*	1080 ℃x 4 hr. + 870 ℃x 4 hr.*
Condition C	1250 ℃x 1.5 hr.*	1080℃ x 4 hr. + 870℃ x 4 hr.*
Condition D	1280 ℃x 1.5 hr.*	1080 ℃x 4 hr. + 870℃ x 4 hr.*

* heating rate: 14 ℃/min. in vac..
cooling rate: 30℃/min. in vac..

explore this situation, plastic strain was introduced at room temperature by Vickers indentation on CMSX-4, and then some re-heat treatments summarized in Table II were given in Ar atmosphere. The former and the latter are planned to simulate the process of damage during servicing, and that of recovery as usual in high temperature components, respectively. From another point of view the former can be reproduced by shot-blasting process before the coating [2]. The Vickers indentations with a pyramidal angle of 136 deg. were punched into the CMSX-4 plate specimen, whose surface was within 5 degree from the (100) crystallographic plane, under a load of 1000 kN. The indentations were punched at equal intervals of 300 μm in the 1.5x1.5 mm square region: 5x5 in the longitudinal and transverse directions, respectively. On the other hand, the heating rate during the re-heat treatment was 15℃/min. Hereinafter the condition of reheat treatment will be represented according to the notations in Table II.

The metallographs after the heat treatments are shown in Figures 1 and 2. At the macroscopic level the region associated with different morphology from the surroundings are clearly identified in Figure 1 in the both cases. Note that the geometrical bowl of the indentations was completely polished away. When the material was exposed to the condition D treatment (see Table II, Fig. 1 (b) and Figure 2), local recrystallization has been achieved, which can be confirmed from such a feature in Figure 2 that γ' precipitates align individual orientation in each microstructural unit. This was also confirmed by the X-ray Laue pattern. It is important to note that the recrystallization has begun at the temperature

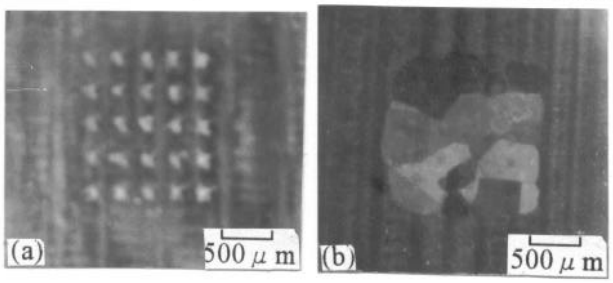

Figure 1: Macroscopic metallographs after the re-heat treatments; (a) at 1220℃, and (b) at 1280℃.

clearly lower than the normal solution heat treatment temperature for the bulk alloy (about 1315 ℃). These results indicate that simple reheat treatment for single crystal alloy subjected to previous plastic strain would be dangerous. In Figure 2 the white precipitates are also found at the grain boundaries, which were identified as being W-rich by using an electron probe micro analyzer (EPMA).

On the other hand, when the condition B treatment was applied, recrystallization is not seen at least at the macroscopic level, and the microstructurally abnormal regions were formed corresponding to the prior indentation traces (Fig. 1 (a)). This transformed region exhibits a cellular structure, which consist of the coarsened γ and γ' precipitates (Figure 2). It is worth noting that the general profile of the transformed region reveals a shape of pollygonization, suggesting that this would be a recovery process accompanied with strain energy release. The shape of the cells is equi-axied at the center and lamellar at the interface of the transformed/normal regions, respectively (Figure 2). These geometries must result from the influence of stress fields due to the indentation [10]. Some researchers have been also confirmed the same type of transformations as Figure 2 in Ni-base superalloys [2-5]. Depending on their research background, they call them "reaction zone", "cellular colony", "cellular precipitation" and "cellular recrystallization". In the present work they will be called "cellular transformation", and will be the focus of this work.

It is worth noting that morphological changes occur drastically between Figs. 1(a) and (b). In order to study this change, differential thermal analysis during the heating process was carried out in the sample in which the 5x5 Vickers indentations were introduced; Figure 3. For the analysis a TGD 9600 (Shinku-Riko Co., Japan) was used, in which an Al_2O_3 block was employed as a reference. The heating rate was 40℃ /min up to 800℃, and 15℃ /min between 800-1320℃. In Figure 3 a clear exothermic reaction is found to occur at about 1250 ℃, which may corresponds to the γ' solvus [6]. A comparison between Figure 3 with Figure 2 indicates that once γ' precipitates are re-solutioned the local recrystallization developed dramatically. A gradual exothermic reaction which can be seen between 1050℃ and 1250 ℃ in Figure 3, must correspond to the microstructural change as shown in

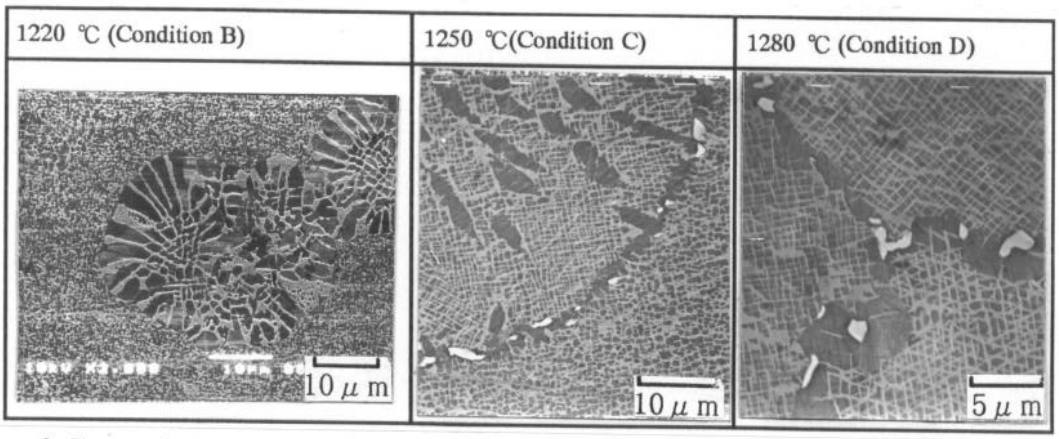

Figure 2: Change of microstructure with the reheatimg temperature in CMSX-4 (Reheating time in 1.5 hrs.).

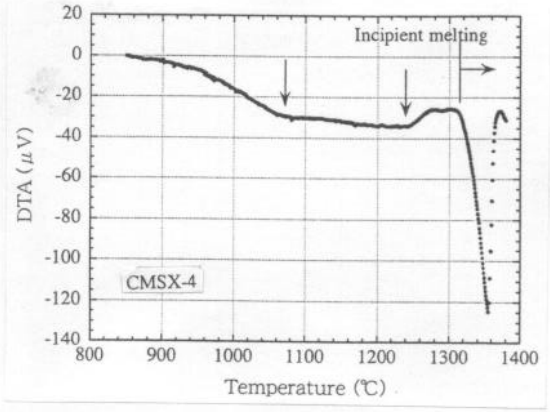

Figure 3: The results of differential thermal analysis (CMSX-4).

and (111) planes, and then the re-heat treatment B was performed (heated at 1220℃ for 1.5 hrs., then aged at 1080℃ for 4 hrs. and at 870℃ for 4 hrs.).

Micrograghs around the indentation before and after the re-heat treatments are summarized in Figure 4. It is found that after the indentation the characteristic slip pattern are activated depending on the crystallographic planes. What is the most exciting in Figure 4 is that the nucleation exhibits a significant crystallographic anisotropy: the predominant directions are <110> directions on the (001) plane indentation, [100] directions on the (011), and <112> directions on the (111) plane, respectively. It is worth noting that the predominant direction was strongly dependent on the crystallographic indentation plane. The mechanism on the anisotropy will be discussed later.

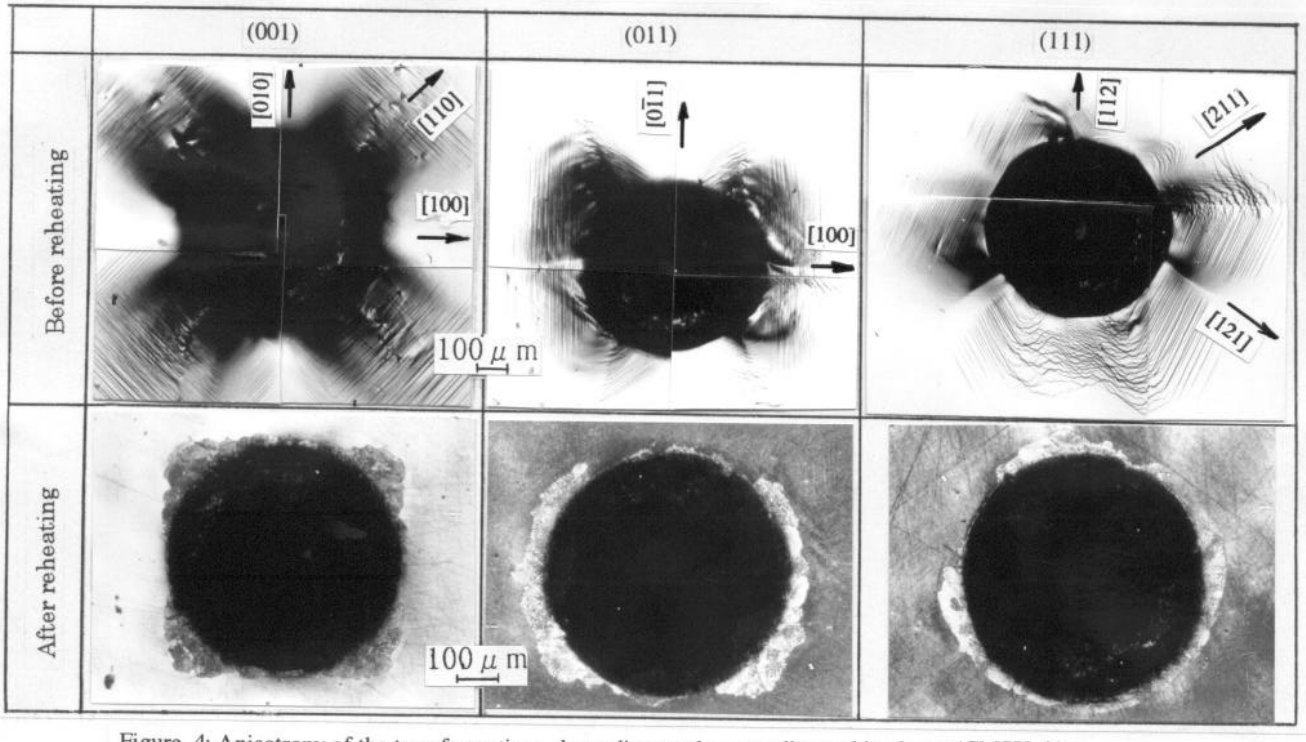

Figure 4: Anisotropy of the transformation, depending on the crystallographic planes (CMSX-4).

Figure 2.

Characteristics of Cellular Transformation

Nucleation and Anisotropy of Cellular Transformation.

Since stress and strain fields are singular at the pyramidal corner of Vickers indention, the cellular transformation should have predominantly nucleated there. This was confirmed experimentally in the previous section. In the other words, it is difficult to study on the anisotropy in the nucleation and development of the cellular transformation, by the procedure employing the Vickers indentation. In order to avoid this problem, a Brinell indenter with a sphere tip whose radius was about 400 μm was employed, and the plastic strain was introduced at room temperature on some crystallographic planes of CMSX-4; planes within 5 degree from (001), (011)

Relation between γ' Rafting and Cellular Transformation

The rafting phenomenon [9] is famous as a morphological change of γ' precipitates. In order to discuss the relation between γ' rafting and the cellular transformation, the microstructure around the Brinell indentation after the re-heat treatment A (see Table II) was observed: Figure 5. The region accompanied with the rafting can be identified independently, neighboring to the cellularly transformed region. This implies that there is a difference between them.

The volume fraction of the γ' phase in the cellularly transformed region is compared with that in the rafted and in the bulk areas (Figure 6). On the measurement the transformed region was classified into two parts: equi-axed

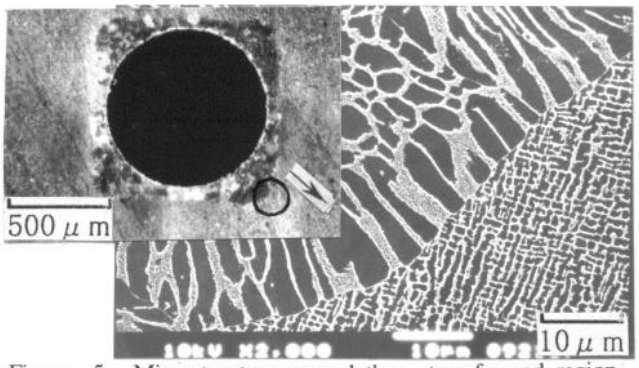

Figure 5: Microstructure around the transformed region (CMSX-4). Indented on (001), and then exposed to the re-heat treatment A in Table II.

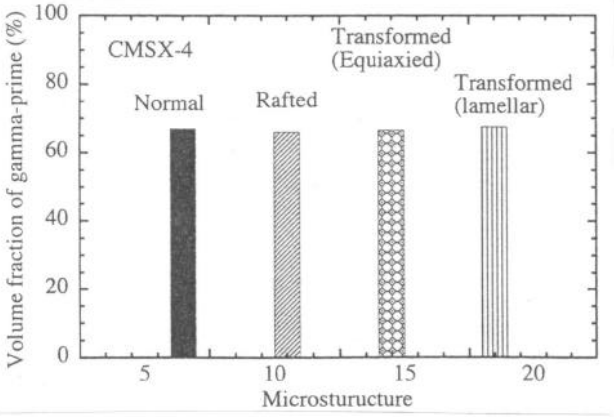

Figure 6: Comparison of γ' volume fraction in the cellular transformed region with that in the other regions (CMSX-4).

region at the center and lamellar region near the interface. No significant differences are found in Figure 6 at any areas, although the measurement at the lamellar region possibly involves large scatter due to their highly elongated, or anisotropic morphology. From these observations it is reasonable to consider that the cellular transformation is different from in some aspects but similar to the rafting phenomenon in other ones.

Effect of Microsegregation on the Cellular Transformation.

The indentation methods employed in the previous section is not always suitable to quantitatively clarify the criterion under which the cellular transformation is developed, because the plastic strain distribution has a high gradient around the indentation. Thus, a uniform distribution must be better. Bi-axial, or tri-axial plastic straining is preferable to uniaxial one, because the actual components generally experience the former type deformation. In order to realize this, cold working was applied to the cylindrical specimen of CMSX-4 as illustrated in Figure 7, by die forging at room temperature. The total strain in the radial direction by this method is about 8.3 % in compression. After die forging the material was exposed to the re-heat treatment C (see Table II).

Metallographs in the longitudinal and transverse sections of

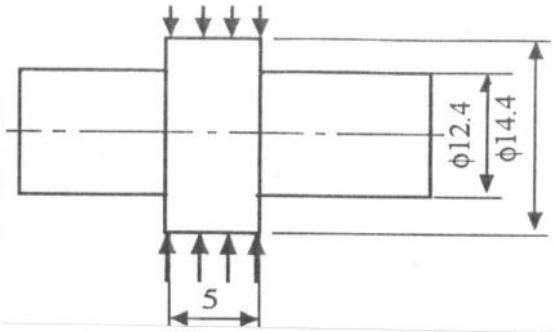

Figure 7: Geometry of specimen die-forged at room temperature.

the sample are given in Figures 8(a) and (b). It is found that while the surface region has been fully recrystallized (Figure 8(c)), the midsection has been partially recrystallized (Figure 8(d)). At the sample core any drastic morphology changes have not occurred (but the loss of γ/γ' coherency) (Figs. 8(a) and (b)). The above inhomogeneous morphological changes may be resulted from the gradient of plastic strain introduced by die-forging. It is worth noting that the inhomogenity of local recrystallization at the mid-section of the sample (Figs. 8(a), (b) and (d)): the local recrystallization grows predominantly along the dendritic core under the same plastic strain.

The EPMA measurement on the distribution of the main chemical elements along the arrow mark in Figure 8(d) is shown in Figure 9. It is found that whereas the γ-side elements (e.g., W, Cr, Co) are relatively rich at the dendritic core, the γ'-side elements (e.g., Al, Ti, Ta) are rich at the interdedritic region, respectively. This result indicates that microsegregation, which depends on the distribution coefficient on phase diagram during the solidification process and on the post-solidified heat treatment(s), play an important role in the preceding inhomogeneous recrystallization.

Relation between Cellular Transformation and Actual Engineering Damage. Does the cellular transformation appear only when the plastic deformation is applied by the Vickers or Brinell indentations ? In order to explore this, the re-heat treatment C was exposed to the CMSX-2 specimen which had been previously subjected to the following three kinds of actual engineering damages: one was due to fatigue at 600℃ [7], the second was due to so-called creep-fatigue loading with hold time on the tension side at 950 ℃ [8], and the third was due to the thermo-mechanical fatigue between the temperature of 400-900 ℃ under the out-of-phase condition. All the damage was introduced into the CMSX-2 specimens in air under uni-axial loading condition, where the specimen axis laid within 5 degree from <001> direction. The experimental details are given elsewhere [7,8].

The metallograph near the crack face of the CMSX-2 specimen is given in Figure 10 (a), that had been previously subjected to the fatigue crack propagation test at 600℃ and then re-heated under the condition C treatment (i.e., reheated at 1250℃ for 10 hrs, and then aged at 1080℃ for 4 hrs,

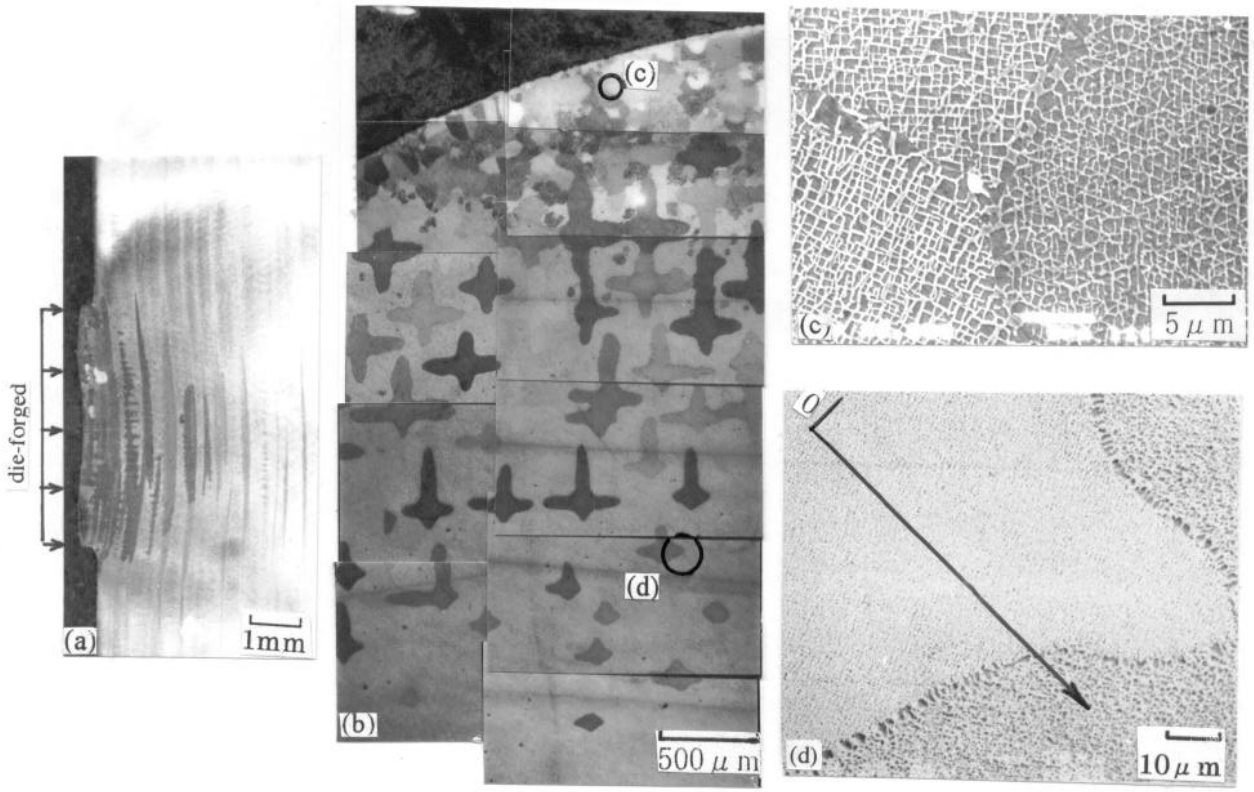

Figure 8: Metallographs of the sample die forged at room temperature, and then reheated by the treatment C (CMSX-4). (a) longitudinal section, (b) transverse section, (c) microstructure near the surface, (d) microstructure inside the sample

followed by aged at 870℃ for 4 hrs.) During the prior fatigue process the fatigue crack had initiated at the center portion perpendicular to the loading axis and then propagated along the crystallographic {111} slip planes [7]. It is found from Figure 10 (a) that the cellularly transformed region is found to be developed along the fatigue fracture surface, and does not develop apart from there, after the reheat treatment. The transformation seems to grow along the dendritic core, which may be due to the effect of microsegregation (see the previous section). The same phenomenon can be seen along the crack plane in the specimen which had been previously exposed to the thermo-mechanical fatigue damage, as shown in Figure 10(c). It is worth noting that the cracks in both cases were propagated mainly by the activation of $\{111\}\langle 1\bar{1}0\rangle$ slip system, which can be identified by the shearing phenomenon of the γ' precipitates [7].

On the other hand, no cellular transformation was found to occur in Figure 10(b), in which the CMSX-2 was exposed to the creep-fatigue damage. Instead, the γ' rafting is observed near the fracture surface, which had been already confirmed before the reheat treatment [8]. In this case the $\{100\}\langle 1\bar{1}0\rangle$ system may be activated more predominantly than the $\{111\}\langle 1\bar{1}0\rangle$ [12].

These experimental results indicate that the cellular

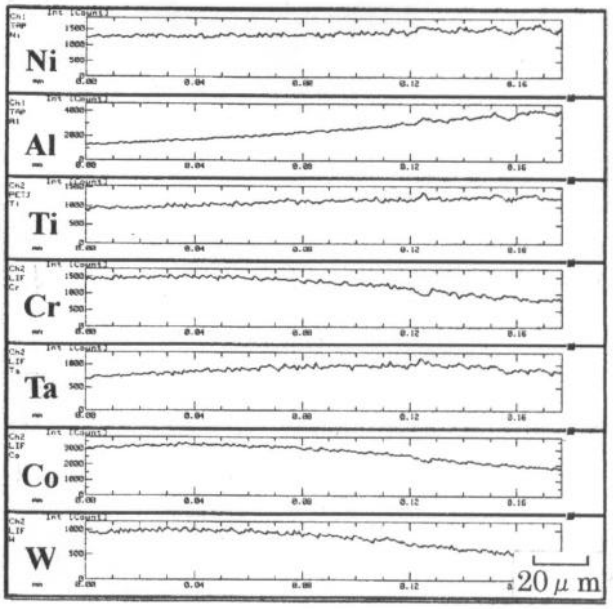

Figure 9: Microsegregation of the main elements in the dedritic structure (CMSX-4).

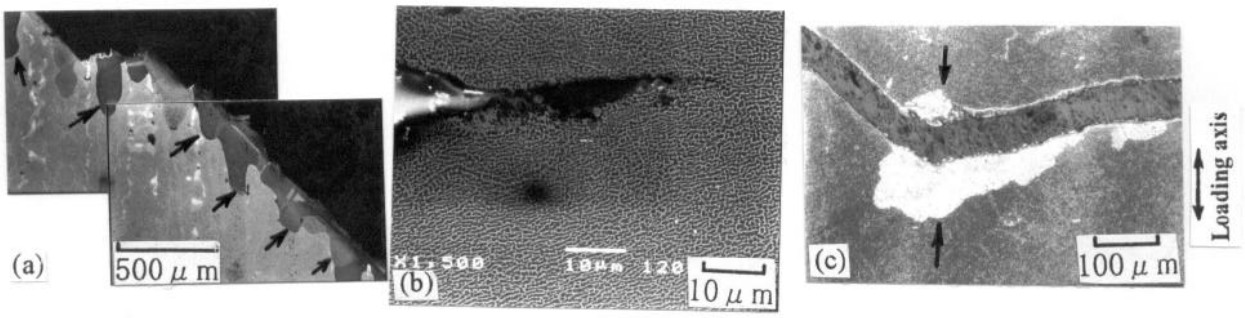

Figure 10: Metallograph of the CMSX-2 primarily subjected to; (a) fatigue damage at 600℃, (b) creep-fatigue damage with hold time on tension side at 950 ℃, and (c) thermo-mechanical fatigue damage between the temperature of 400-900 ℃ under the out-of-phase condition, followed by the reheat treatment, C.

transformation can be realized in actual components. Furthermore, the above features strongly suggest that the cellular transformation must originate only when the inelastic strain inducing the shearing of γ' precipitates is introduced. The experiments obtained in earlier sections support this interpretation. It is also important to note that this appeal could be a potential tool for failure analysis.

Effects of Cellular Transformation on Small Fatigue Crack Propagation at High Temperature.

It is not difficult to suppose that once the cellularly transformed region is formed in single crystal Ni-base superalloys, it is harmful for the high temperature strength, because single crystal alloys are generally free of grain boundary strengthened elements. The effect of local cellular transformation on fatigue strength is investigated in this section. For the experiments, solid cylindrical smooth specimens with locally cellular transformed areas were prepared, according to the following procedures: after the cold working was applied to the CMSX-4 specimen with same geometry and by the same procedure as Figure 7 at room temperature, the re-heat treatment C was performed, followed by the machining into the solid cylindrical smooth specimen of which gauge section diameter and length were 5 mm and 13 mm, respectively. At the center of the specimen gauge section a transformed region was formed over about 5 mm in length (See Figure 6). The fatigue tests were carried out at 950 ℃ in air at a frequency of 10 Hz under a load ratio of -1.

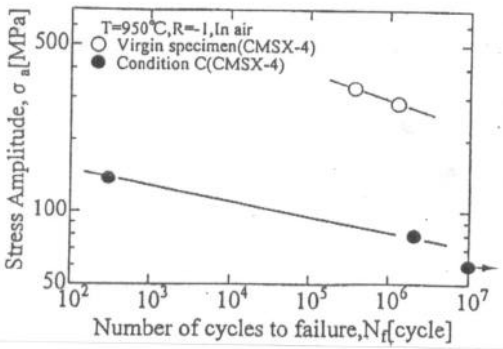

Figure 11: Comparison of the fatigue lives between the locally transformed and the bulk materials at 950 ℃ (CMSX-4).

Figure 11 is a comparison of the fatigue lives between the locally transformed and the bulk materials, which indicates the former exhibits the fatigue strength remarkably lower than the latter. This is a direct evidence indicating the seriousness of the problem.

As already shown in Figure 2, the cellularly transformed region reveals some different morphologies depending on the re-heat treatments. The effect of the morphology on the small fatigue crack propagation is a next project. For this purpose a 5x30x1.5 mm plate specimen with a locally transformed region with different morphologies was prepared: after Vickers indentation was punched into the CMSX-2 plate, the heat treatments; B and D, were carried out, followed by the polishing until the geometrical bowl of the indentation completely disappeared. Any mechanical notches were not introduced in the specimen. The transformed region whose size was about 0.4x0.4 mm in area and 50 μm in depth, respectively, existed at the center portion of the plate specimen. The specimen axis lies within 5 degree from the <001> direction. The small fatigue crack propagation tests were carried out at 950 ℃ in air at a frequency of 10 Hz under a load ratio of 0.05. The naturally initiated surface small fatigue crack growth was monitored, by periodically replicating the specimen surface. The small crack length measured was about from 20 μm to 200 μm.

Figure 12 shows a small fatigue crack in the smooth specimen with a locally cellular transformed region, which indicates that predominant crack initiation is from the transformed/normal interface. The propagation rates of these naturally initiated small cracks are compared with those in the bulk material in Figure 13, as a function of stress intensity factor range, ΔK, where ΔK was evaluated from the Raju-Newman equation by assuming a semi-circular geometry for the surface cracks [13]. The data points in the Figure exhibit the rates of multiple small cracks near the transformed region, which were obtained by using multiple specimens. From the Figure it is found that the small cracks near the transformed region exhibit the rates significantly higher than those in the bulk material, and they generally grew at lower ΔK level. It is important to note that this trend can be seen not only in the cracks running at the locally recrystallized area (which was exposed to the re-heat treatment D) but also in the cracks running at the cellularly transformed area. These experiments show that it is a serious concern from industrial point of

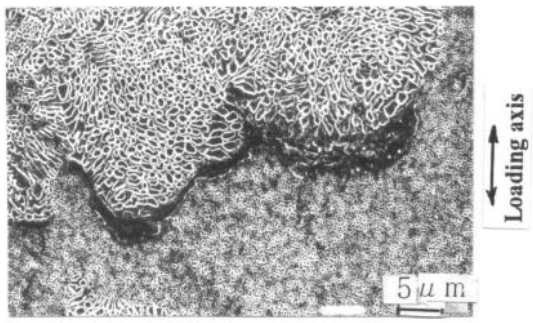

Figure 12: A fatigue crack nucleated in the CMSX-4 specimen with a locally cellular transformation region.

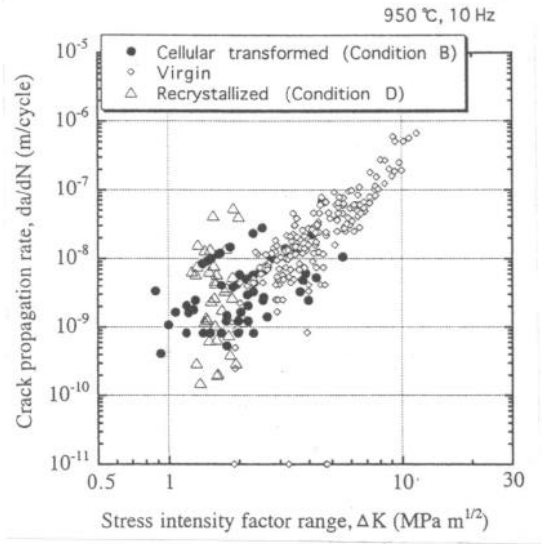

Figure 13: Small fatigue crack propagation in the CMSX-2 specimen with a locally cellular transformed region.

view to get understanding on the transformation and to develop the prevention method.

Discussion

Nucleation of Cellular Transformation.

It is natural to suppose from the results of the previous section that the main driving force for the cellular transformation should be strain energy stored in the material [2-4]. On the other hand, the nucleation of the cellular transformation was found to reveal significant anisotropy, in which the shearing of γ' precipitates resulting from the activation of $\{111\}\langle 1\bar{1}0\rangle$ system may play an intrinsic role. Thus, let's consider the slip system activated in the Brinell indentation process.

The stress field around the Brinell indentation can be modeled and analyzed by applying the famous analysis on a sphere cavity expanding in infinite body. The stress components at the surface of the cavity, or Brinell indentation, are expressed by

$$\sigma_{rr} = -p$$
$$\sigma_{\theta\theta}=\sigma_{\phi\phi}= p/2 \qquad (1)$$

where p is a internal pressure. The r, θ and ϕ are in spherical coordinates, which are taken with reference to the specimen into which the Brinell indentations is punched (see Figure 14). These stress components are converted to σ_{ij} (i,j =1,2,3) on the basis of crystallographic cubic axis (see Figure 14), through the tensor transformation:

$$\sigma_{ij} = l_{si} l_{tj} \sigma_{st} \qquad s, t = r, \theta, \phi \text{ and } i,j = 1,2,3 \qquad (2)$$

where l_{si} and l_{tj} are the directional cosine between the two sets of coordinate axes. Based on Eqs. (1) and (2) the shear stresses, τ, on the twelves series of $\{111\}\langle 1\bar{1}0\rangle$ slip systems can be determined. It is natural to consider that the slip system accompanied with the maximum τ value, τ_{max}, of all the slip systems should be primarily activated at a given point.

The distribution of the τ_{max} normalized by the indentation pressure, p, is illustrated in Figure 15, together with the primary slip system activated, where the calculation was performed for $\theta=\pi/3$ rad. (See Figure 14). Figure 15 is illustrated so that the value of τ_{max} corresponds to the distance from the origin. Note the specific τ_{max} distribution dependent on the crystallographic indentation planes: 4-fold symmetric axes on (001) indentation, 2-fold ones on (011), and 3-fold ones on (111), respectively. There is an interesting relationship between these symmetries and the profile of the cellular transformation given in Figure 4.

Comparing Figure 15 with Figure 4, at first, note a common feature that the nucleation sites always involve the site where the most dominant slip system is changed from one to another in all the cases: e.g., [112] and [211] directions in the (111) indentation, [110] and $[\bar{1}\bar{1}0]$ directions in the (001) indentation, and [100] and $[0\bar{1}1]$ directions in the (011) indentation, respectively. However, there are some exceptions: e.g., [211] direction in the (111) indentation, [100] direction in the (001) indentation, and $[0\bar{1}1]$ direction in the (011) indentation, respectively. Accordingly the above

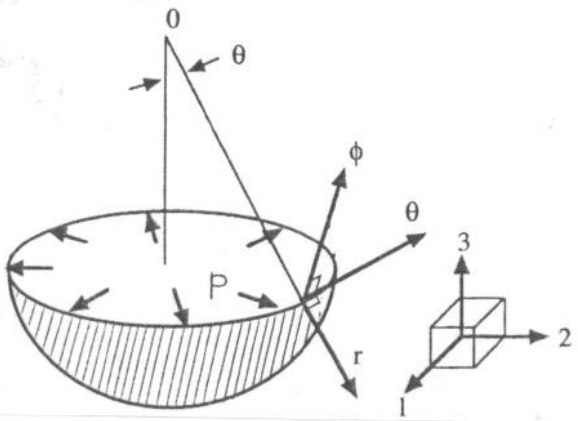

Figure 14: Illustration on spherical coordinates around the Brinell indentation, and the crystal coordinates.

condition is not sufficient. Relating to the nucleation site, the second common feature found in Figure 15 is that the changing ratio in τ_{max} along with orientation (which may correspond to the gradient of stress and strain) is very high at the nucleation site, which seems to be another requirement

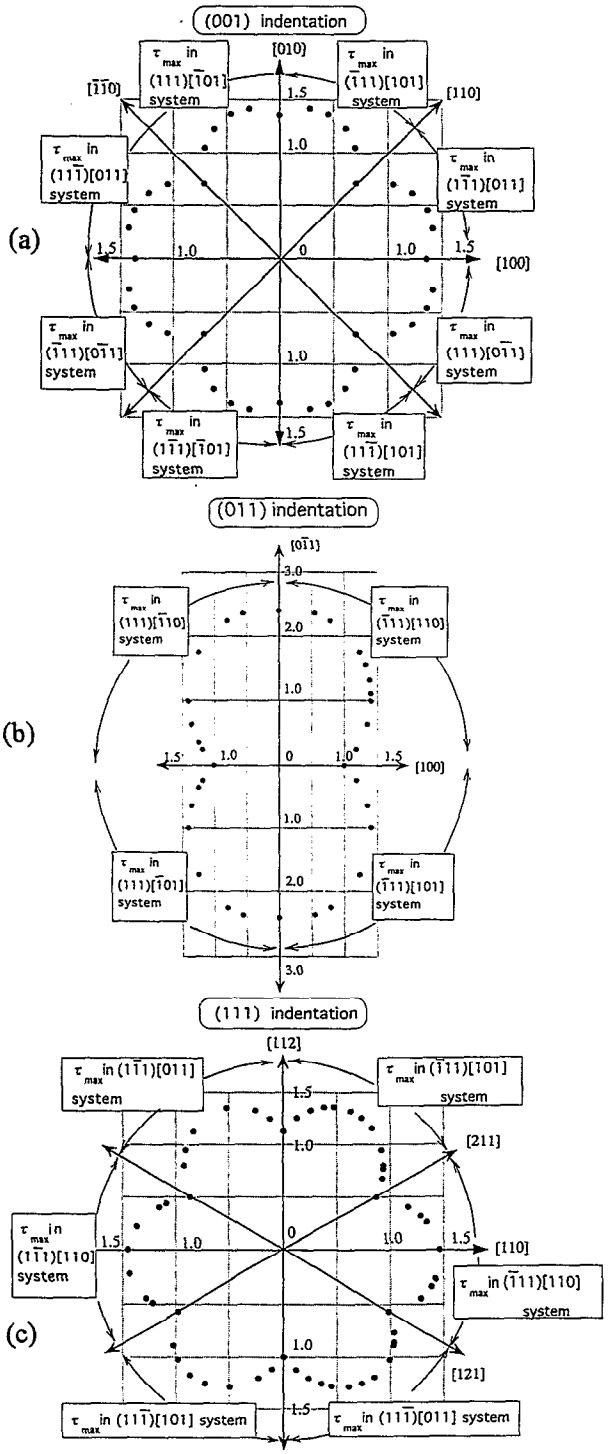

Figure 15: The distribution of the τ_{max} around the Brinell indentation, and the primary slip systems activated.

condition for the nucleation site. Remember that micro shear, or kinked bands where the gradient in stress and strain is very high, is a preferential site for recrystallization in general materials [14]. The reason why the [0$\bar{1}$1] direction in the (011) plane indentation was not the nucleation site (Figure 4) is reasonably explained by the above second condition, because the changing ratio in τ_{max} is very low there. One exception which does not satisfy the second aspect is found in the [211] direction in the (111) indentation. According to the calculation in Figure 15, only slip direction but no slip plane is supposed to be changed between this direction. This would reduce the singularity of stress field there, resulting in non-nucleation there.

Growth of Cellular Transformation.

Regarding as general recrystallization, Johnson-Mehl type equation is famous. The recrystallized ratio, r(t), at a given time, t, is generally expressed by

$$r(t) = 1 - \exp(-At^m) \qquad (3)$$

where A and m are constants, respectively [14]. Employing new constants C and n, Eq. (3) can be converted into

$$R(t) / R_f = 1 - \exp(-Ct^n) \qquad (4)$$

where R(t) and R_f are the size of cellular transformation zone at re-heat treatment time, t, and that finally reached after infinite heat treatment time. The latter would be a function of transformed/bulk interface energy. It is interesting to study the growth of cellular transformation, according to Eq.(4).

The change of R(t) with the reheating time, t, is shown in Figure 16, when the Brinell indention was punched on (001) plane. Because the transformation was highly anisotropic as shown in the previous section (see Figure 4), R(t) was represented and measured by the size between the Brinell circle and the transformed/bulk interface to <110> direction.

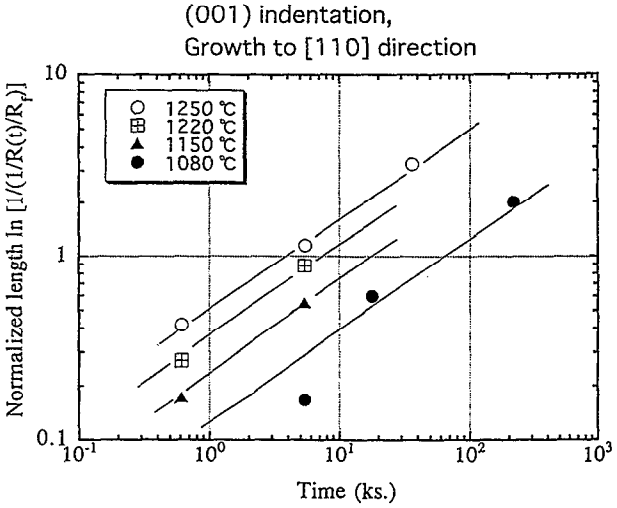

Figure 16: The change of the cellular transformation size with the heat treatment time.

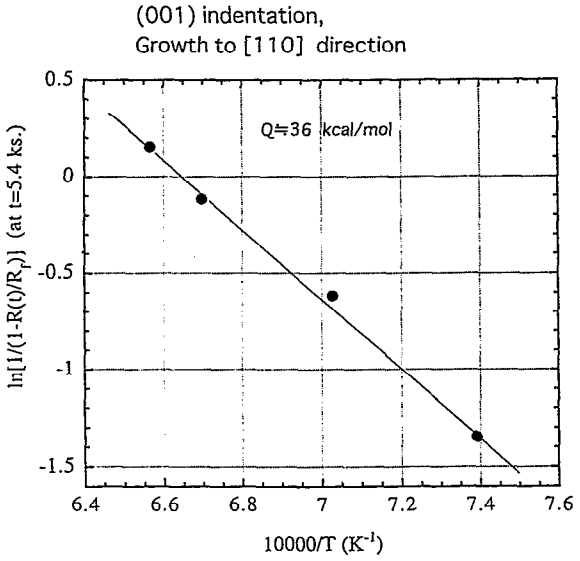

Figure 17: Temperature dependence in the cellular transformation size.

The value of R_f was tentatively approximated by 135 μm. It is found from Figure 16 that the growth can be successfully expressed by Eq. (4). Note that the value of n can be well approximated by 0.5, which indicates that the diffusion was controlling the growth rate.

It is also interesting to investigate the temperature dependence in the transformation, by employing Arrhenius type activation process in the constant, C. The Arrhenius plot at t=5.4 ks. is given in Figure 17, which shows an activation energy of about 36 kcal/mol. The activation energies have been measured 26-28 kcal/mol for Ni self diffusion, and 64 kcal/mol for diffusion of Al atoms in Nickel by other researchers [11]. Interestingly the present value is intermediate between them. This indicates that the cellular transformation must be a diffusion process of Al and Ni atoms.

Conclusions.

The conclusions obtained are summarized as follows:

(1) When CMSX-2 and CMSX-4 were subjected to damages associated with local plastic deformation, followed by the re-heat treatments, the cellular transformation associated with γ/γ' microstructure coarsened in lamellar or equiaxed array was originated. This was not a special phenomenon, but it was actually reproduced in the material subjected to fatigue and thermo-mechanical fatigue damages.

(2) The transformation was originated and developed with high anisotropy, being influenced by the following many factors: i.e., the strain field by the local plastic deformation, the crystallographic orientation, the re-heat treatment temperature and time, and the microsegregation in the material. The γ'-solvus in the reheating process drastically accelerated the local recrystallization.

(3) The shearing of γ' precipitates in the straining process may play an intrinsic role in the cellular transformation: when the {111}<1$\bar{1}$0> systems were activated, the formation was significant. When the {100}<1$\bar{1}$0> slip systems were activated such as in creep failure at higher temperature, on the other hand, it was negligible.

(4) The growth of the transformation was successfully represented by the Johnson-Mehl type equation. The growth of the transformation must be controlled by diffusion process of Al and Ni, where activation energy was determined by about 36 kcal/mol.

(5) The small fatigue crack propagation rate was remarkably enhanced at the transformed region.

Acknowledgement:

Financial supports by the Ministry of Education, Japan, as Grant-in-Aid for Scientific Research (No: 10550097) and by Zairyo-Kagaku Foundation are greatly acknowledged.

References

1. For example, J. Stringer and R. Viswanathan, "Gas Turbine Hot Section Materials nd Coatings in Electric Utility Applications", (Paper presented at *ASM 1993 Congress Materils Week, Pittsburgh, 1993)*, 1-8.

2. S.D.Bond and J.W.Martin, Surface Recrystallization in A Single Crystal Ni-based Superalloy, J. Mater. Sci., 19, (1984), 3867-3872.

3. A Porter and B. Ralph, The Recrystallization of Ni-base Superalloys, J. Mater. Sci., 16, (1981), 707-713.

4. P. Portella, Influence of Cellular recrystallization on the fatigue Behavior of Single Crystal Ni-based Superalloys, " MicroStructure and Mechanical Properties of Metallic High Temperature mnaterials, Eds. by H. Mughrabi, DFG, (1999), 441-453.

5. W.S. Walston, J.C., Schaeffer and W.H. Murphy, Super-alloys '96, A New type Microstructural Instability in Super-alloys -SRZ, (1996), 9-18.

6. U. Paul and P.R. Sahm, Inhomogenities in Single Crystal Components, Mater. Sci. & Engg., A173, (1993), 49-54.

7. M. Okazaki, H. Yamada and S. Nohmi, Temperature Dependence of the Intrinsic Small Fatigue Crack Growth Behavior in Ni-Base Superalloys Based on Measurement of Crack Closure, Metall. & Mat. Trans., 26, (1996), 1021-1033.

8. M. Okazaki, Creep-Fatigue Small Crack Propagation of a Single Crystal Ni-Base Superalloy: Microstructural and Environmental Effect, Int. J. Fatigue, 20 (1999), 79-86.

9. F,R,N. Nabarro, Rafting in Superaloys, Metall. Trans., 27-A, (1996), 513-530.

10 A. Pineau, Influence of Uniaxial Stress on the Morphology of Coherent Precipitates During Coarsening, Acta Met., 24, (1976), 559-567.

11. K. Smidoda, W. Gottschalk and H. Gleiter, Diffusion in Migrating Interfaces, Acta Met., 26, (1978), 1833-1836.

12. For example, V. Paidar, D.P. Pope and V. Vitek, A Theory of the Anomalous Yield Behavior in $L1_2$ Ordered Alloys, Acta. Met., 32, (1984), 435-448.

13. I.S.Raju and J.C. Newman: Eng. Frac. Mech., 11, (1979), 817-827.

14. For example, F.J. Humphrey and M. Hathery, Recrystallization and Related Annealing Phenomena, (Pergamon Press, 1995).